Draft version September 4, 2026
Typeset using LaTeX default style in AASTeX631

Continuous Modulated Waves from Jupiter
A Possible Signature of Rotating Shells with Distinct Periods Inside Jupiter

Herbert Weidner [1]

[1] *University of applied sciences, Aschaffenburg, Germany*

Abstract

We report the detection of continuous microhertz waves originating from Jupiter, recovered from two decades of atmospheric pressure measurements across Germany. Barometers act as large-aperture antennas for low-frequency signals, allowing coherent recovery of a carrier near 55.97 μHz, which corresponds to twice the rotation frequency of Jupiter's solid core. A direct-conversion receiver iteratively compensates all known phase modulations caused by Earth's orbit and the four Galilean moons, concentrating the wave's energy into a narrow spectral line with a signal-to-noise ratio of 100. We measure the long-term frequency drift of Jupiter's core and determine the modulation indices associated with each moon. The phase-modulation pattern is stable across 318 independent realizations. Additional spectral features indicate that Jupiter hosts multiple internal oscillators with distinct frequencies. These results demonstrate that Earth's atmosphere responds coherently to microhertz waves generated by nearby planets.

Keywords: Jupiter (873), Natural satellite dynamics (2212), Gravitational interaction (669), Computational astronomy (293)

1. INTRODUCTION

Planets and their satellites generate tidal deformations that propagate through the Solar System and can, in principle, influence Earth's atmosphere. Standard tidal catalogs, such as Hartmann+Wenzel (1995), list thousands of static components derived from astronomical arguments, but they implicitly assume that the planets themselves remain rigid. In reality, giant planets are periodically deformed by their moons, which implies that their gravitational influence on Earth may vary on timescales of hours to days.

Jupiter is a particularly compelling case. Its three inner Galilean moons form a 4:2:1 Laplace resonance that forces the planet – at least its cloud layer – into a continuously changing, non-axisymmetric shape. If these deformations are sufficiently strong, they should generate time-dependent gravitational signatures detectable in long-term atmospheric pressure records on Earth.

Microhertz waves remain largely unexplored because no dedicated instruments exist for their detection and because conventional Fourier methods fail when the signal is deeply buried in atmospheric noise. Nevertheless, barometric pressure data contain subtle imprints of external forcing. Jupiter's rotation period of 9.925 hours corresponds to expected wave frequencies near 27.99 μHz and 55.97 μHz. These frequencies are not visible in standard FFT spectra, likely because the signals are weaker than the atmospheric noise floor and strongly Doppler-shifted by the nonlinear Earth–Jupiter orbital motion. Additional phase modulations arise from the orbital motion of the four Galilean moons, distributing the wave's energy across a wide set of sidebands.

In this work, we show that these frequencies become accessible through coherent processing of multi-year atmospheric pressure data. By iteratively reversing the phase modulations caused by Earth's orbit and Jupiter's moons, we recover the carrier frequency with high signal-to-noise ratio and measure both the long-term frequency drift of Jupiter's core and the modulation indices associated with each moon. The results indicate that Jupiter hosts multiple oscillators with distinct frequencies, concealed beneath its cloud cover.

Several obstacles must be overcome in the process: First, an FFT spectrum is not a substitute for a narrow-band receiver of the kind used in radio astronomy; it reveals only signals that rise clearly above the noise. Second, the uncertainty relation discussed by Küpfmüller (1993) applies: the shorter the measurement interval, the broader the spectral lines become. To achieve

herbertweidner@gmx.de

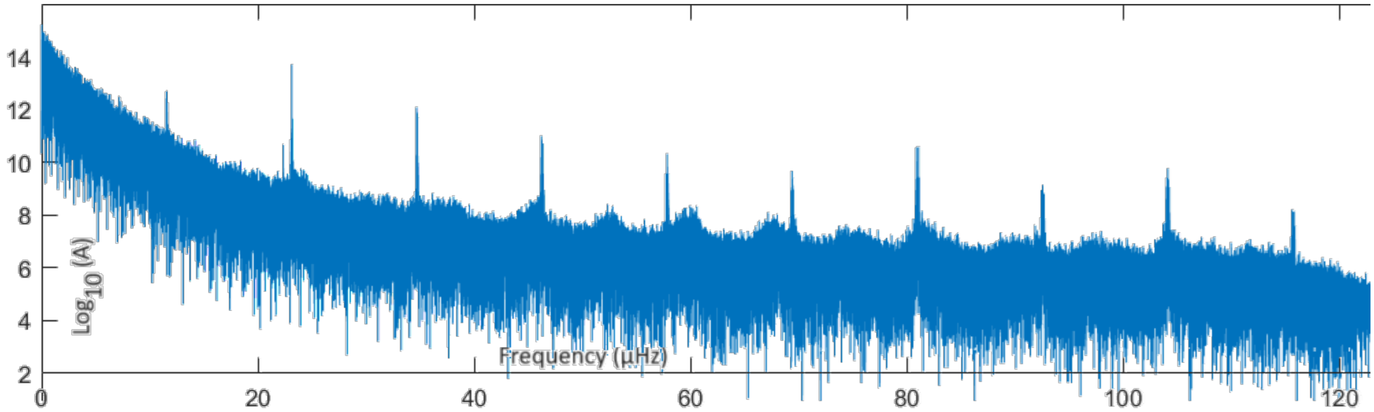

Figure 1. Power spectrum of atmospheric pressure, using one measurement per hour. The data represent the mean pressure across Germany from 2000 to 2020. The spectrum is dominated by broadband atmospheric noise, and no identifiable signal near Jupiter's expected rotation frequencies (28 or 56 μHz) is visible.

a frequency resolution of 10 nHz, the distance between Jupiter and Earth would have to remain constant for three years. Because both planets move nonlinearly, the Doppler effect further ensures that the received frequency is continuously changing.

A fourth reason prevents the total wave energy from being concentrated in a single spectral line: the four Galilean moons, with orbital periods of only a few days, force Jupiter – and especially its cloud envelope – into a complex pirouette around the system's barycenter. As a result, Jupiter emits a phase-modulated wave whose total energy is distributed across multiple spectral lines (spread spectrum). Initially, we assumed that the moons would barely move the massive Jupiter and would therefore produce only weak phase modulation (PM).

For this reason, we analyzed both frequencies with a narrow bandwidth to suppress unnecessary noise and found the following:

– Only at 55.97 μHz does a signal with sufficient amplitude exist. All results refer to this frequency.

– The innermost moon, Io, produces an unexpectedly large modulation index η. At first, this index could be determined only imprecisely, because too narrow a BW distorts the modulation and introduces measurement errors. After gradually widening the BW, the final result (Fig. 2) shows that the sidebands of Jupiter's wave extend over a surprisingly broad frequency range.

Since the sidebands carry far more energy than the carrier frequency at 56 μHz, one loses a substantial amount of information if one focuses only on individual spectral lines. Our goal is to extract the full information content arising from the interplay of all lines. This can only be achieved with a method that also accounts for the phase relationships among the sidebands.

In this work, we demonstrate that Jupiter's wave can be extracted from 20 years of barometric measurements by coherently reversing the phase modulations caused by the Earth's orbit and the four Galilean moons. Using a homodyne detection scheme with extremely narrow bandwidth, we recover the carrier frequency with a signal-to-noise ratio of $\sim$100 and measure both the long-term frequency drift of Jupiter's core and the modulation indices associated with each moon. The resulting phase-modulation pattern is stable across 318 independent realizations and confirms that Earth's atmosphere responds coherently to microhertz waves.

2. THE RECEPTION PRINCIPLE FOR PHASE MODULATION

The structure shown in Fig. 2 occupies almost the same frequency range as the overall spectrum in Fig. 1, but it is not recognizable in the noise. It is not promising to attempt to measure the exact frequencies, phases, and amplitudes of all sidebands (below the noise level!) and reconstruct the original signal from them. In high-frequency engineering, when one wants to detect weak signals of known frequency, PM is always used: before transmission, the sender distributes the total energy over many known sideband frequencies with defined phases. If the PM is undone in the receiver, the many sidebands disappear and the total signal energy is concentrated in a narrow spectral region around the carrier frequency; the amplitude increases due to constructive interference. Interfering signals and noise may cause short-term disturbances, but they do not affect the amplitude in the long term. We note that the following program exclusively demodulates PM and does not respond to amplitude modulation (AM). We will discuss the latter in Section 9.

To detect Jupiter's wave signal, we apply a method that can be described – simplified – as follows:

a) Jupiter transmits at f_{wave} = 55.97 μHz a signal that is buried in the noise (Fig. 1). Our 'antenna' is a randomly chosen subset of a total of 115 barometers.

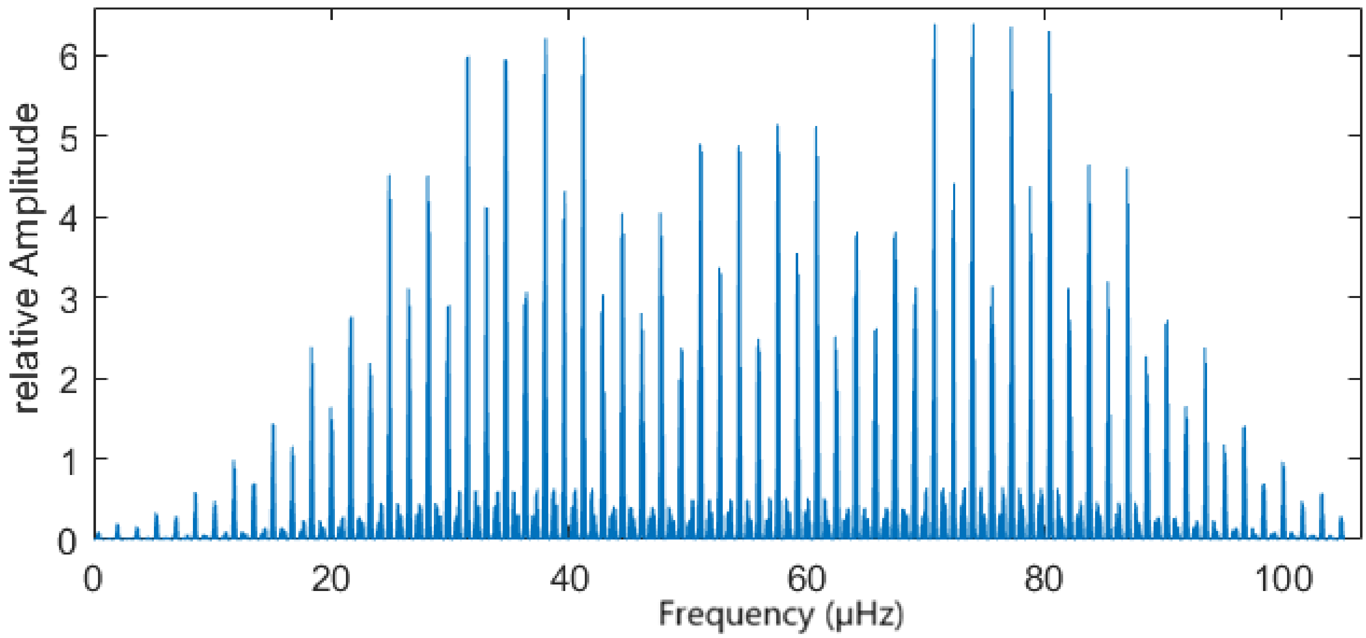

Figure 2. Spectrum of Jupiter's wave after partial demodulation. The 4:2:1 orbital resonance of Io, Europa, and Ganymede produces the characteristic multi-line structure. Callisto and the slow orbital motion of Earth generate the small perturbations along the lower edge. The unusually broad distribution of sidebands reflects the strong phase modulation imposed by the inner moons.

b) We phase-modulate a local oscillator of slightly offset frequency f_0 with the known orbital frequencies of the Galilean moons.

c) We multiply (mix) f_{wave} und f_0, filter the difference signal f_{IF} with an extremely narrow bandwidth, and measure the amplitude and drift of the carrier frequency.

d) We adjust the amplitudes and phases of the modulation frequencies of the local oscillator with the goal of maximizing the carrier amplitude. The criterion is a steady increase in amplitude. We allow tiny corrections to the orbital frequencies (on the order of 10^{-11} Hz), since the moons' orbital periods are known.

e) We repeat steps b–c–d until the changes become negligible. At that point, the PM of the local oscillator and the wave are identical (Fig. 2). We store the results and repeat the procedure with data from other barometers.

In the following, we discuss each individual step in detail.

3. DATA SOURCE

Data Acquisition: We use Earth's atmosphere as an antenna, since it is influenced by the planet Jupiter. Barometers serve as sensors that convert pressure fluctuations into usable measurements. Atmospheric pressure data were obtained from the Deutscher Wetterdienst (2021), comprising hourly measurements from more than 115 barometric stations across Germany between 2000 and 2020. Only stations with at least ten years of continuous operation were included.

The expected wavelength of the signal ($\lambda > 10^{12}$ m) is far larger than Earth's diameter. This has two consequences: the spacing between barometers is irrelevant, and all sensors 'breathe' in phase. Thus, when the records of two sensors are added, the amplitude of any continuous signal doubles.

Sensor Calibration: All pressure sensors used by the DWD are temperature-compensated and conform to international standards, with a measurement range of 500–1100 hPa and an accuracy of ±0.1 hPa. Instrumental drift and data gaps remain unchanged because they may influence the amplitude of the signal but cannot generate frequency-stable oscillations or phase-modulate them. Data synchronization is accurate to the second and is guaranteed by the DWD.

Sampling: Air pressure is not measured continuously but at fixed intervals of $T_s = 1$ hour. The inverse of T_s is the sampling frequency f_s. Although the signal does not pass through an analog low-pass filter with cutoff frequency $0.5 f_s$, aliasing effects are practically eliminated when sampling atmospheric pressure hourly.

Validation Dataset: Our goal is to detect waves from Jupiter using many independent long-term barometric time series. In the DWD archives, only very few barometers have recorded continuously over a full 20-year interval. However, numerous 10-year data segments exist. For the period 2000–2009, we identified 64 suitable time series; for 2010–2019, we found 51.

The signal amplitude in a single barometer record is insufficient for an unambiguous detection. A reliable signal-to-noise ratio is achieved only when at least 20 independent time series are coherently added. For this reason, we proceed as follows:

From the 64 time series available for 2000–2009, we select 40 and add them coherently, yielding $\sim 10^{17}$ possible combinations. From the 51 time series available for 2010–2019, we again select 40, resulting in $\sim 10^{10}$ possible combinations.

Linking the two 10-year chains produces a combined 20-year dataset, which serves as the basis for the search for Jupiter's wave. A potential discontinuity at the connection point is irrelevant, as it cannot generate spurious spectral lines.

The probability that two resulting data chains are structurally similar is extremely small.

4. SIGNAL PROCESSING

We must avoid any influence from nearby frequencies when measuring the amplitude of Jupiter's wave carrier, and therefore we filter with an extremely narrow bandwidth. It would be incorrect to simply cut off the sidebands, which carry most of the total wave energy (Fig. 2). Doing so would prevent us from detecting the carrier in the noise and would discard all evidence that Jupiter actually transmits the carrier frequency. Our approach is to first undo all phase modulation so that the energy contained in the sidebands is shifted back into the carrier frequency, and only then apply narrow-band filtering.

The solution is a direct-conversion receiver: we modulate a local oscillator at frequency f_0 in exactly the same way as the wave we expect from Jupiter – same frequency, same drift, same phase, at every moment in time. We begin with the usual approach:

$$y = sin(2\pi t \cdot f_0 + \phi_{modulation}) \tag{1}$$

and adjust the two parameters f_0 and $\phi_{modulation}$ to the problem: The frequency f_0 can change proportionally to time and $\phi_{modulation}$ can be the sum of several sine functions – a different one for each planet. In the simplest case, the modulation consists of a single frequency f_{mod} and the equation is

$$y = sin(2\pi t(f_0 + t\dot{f}) + \eta \cdot sin(2\pi t f_{mod} + \varphi)) \tag{2}$$

A sinusoidal PM causes the instantaneous frequency of the signal to fluctuate periodically between the limits $f_0 + \Delta f$ (maximum blue shift) and $f_0 - \Delta f$ (maximum red shift). The quantity Δf is referred to as the frequency deviation. The instantaneous frequency at a given point in time is difficult and inaccurate to measure, as it is never constant over a longer period of time. It is easier and more common to determine the modulation index η using equation (2) and calculate $\Delta f = \eta \cdot f_{mod}$.

Multiplying the oscillator output y with a signal of frequency f_{wave} yields

$$A sin(f_{wave}) sin(f_0) = \frac{A}{2}(cos(f_{wave} - f_0) - cos(f_{wave} + f_0)) \tag{3}$$

The second term, $cos(f_{wave} + f_0)$ is irrelevant and is removed by a low-pass filter. The better the imitation of the incoming signal, the closer the mean value of the first term, $cos(f_{wave} - f_0)$, approaches unity. This remains true even when both frequencies change synchronously.

A filter with an extremely narrow bandwidth of about 1 nHz and a sampling frequency of 3600^{-1} Hz is technically feasible, but it requires very long computation times. A faster approach is to decrease the sampling frequency by a factor of 64, decimate the file length accordingly, and then apply a windowed sinc filter. The bandwidth must not be too small, because we still need to determine the frequency drift of the wave.

A major challenge in these measurements is the strong phase modulation caused by the planet Io. Its orbital period of 42.46 hours corresponds to a modulation frequency of $f_{mod} \approx 6.545\ \mu$Hz. The measurements yield a modulation index of $\eta \approx 7$, from which the frequency deviation follows as $\Delta f = \eta \cdot f_{mod} \approx 46\ \mu$Hz. As a result, Io causes Jupiter's "transmit frequency" to sweep periodically across the range $11\ \mu\text{Hz} < f_{wave} < 103\ \mu\text{Hz}$ – nearly the entire span shown in Fig. 1.

Using Carson's formula, $B = 2 f_{mod}(\eta + 1)$, the frequency-modulated signal requires a minimum bandwidth of 105 μHz to avoid distortion of the modulation. The carrier frequency of 56 μHz is just sufficient to accommodate this bandwidth.

5. RESULTS

All measurements begin on 2000 January 01. At this epoch, the frequency of Jupiter's wave is

$$f_{wave} = 55.970\,045\ \mu\text{Hz} \pm\ 69\ \text{pHz}$$

The frequency drift follows the relation $\dot{f} = at + bt^2$, with

$$a = (7.7 \pm 2.1) \times 10^{-19}\ s^{-3} \text{ and } b = (-7.9 \pm 2.2) \times 10^{-28}\ s^{-4}$$

Table 1. The phase modulations of Jupiter's wave frequency f_{wave}. From the phase, one can determine the positions of the moons relative to Jupiter, and the position of Earth relative to the Sun, on 2000 January 01. The listed values are the mean results of 318 independent iterations. The records originate from randomly selected barometers.

	Earth	Io	Europa	Ganymede	Callisto
f_{mod}	29.0255 (nHz)	6.54521 (μHz)	3.2582 (μHz)	1.61006 (μHz)	0.6949 (μHz)
±Error (pHz)	0.029	7.9	9.6	8.0	14.7
Index η	2.458	6.939	1.802	3.035	0.130
±Error	0.007	0.007	0.004	0.006	0.005
Phase	2.698	-0.41	-0.171	4.760	3.679
±Error	0.019	0.026	0.014	0.018	0.057
Δf (μHz)	0.07134	45.40	5.87	4.89	0.09

Jupiter's solid surface is invisible. Therefore, the sidereal rotation period (System III) was defined by radio astronomers and corresponds to the rotation of the planet's magnetosphere; its official rotation period is 9.9250 hours (9 h 55 m 30 s). The wave frequency derived from this value (55.9754 μHz) differs significantly from our result.

Jupiter's wave is phase-modulated by at least five distinct frequencies: four moons perturb Jupiter's motion, and the receiving antenna (Earth's atmosphere) orbits the Sun. If we were measuring the wave from a distant binary system, we would observe alternating maximum blue shift ($f_{wave} + \Delta f$) and maximum red shift ($f_{wave} - \Delta f$) at intervals of 365.26 days. Because Jupiter orbits the Sun in the same direction but more slowly, this interval increases to 398.88 days. The expected phase modulation at the corresponding frequency of about 29 nHz can be detected with remarkable precision (Table 1).

The demodulation process removes all sidebands of the wave and produces a substantial increase in the carrier amplitude. Together with Jupiter's relatively small distance, this results in an unexpectedly high signal-to-noise ratio of ~100 (Fig. 4).

6. DIRECTION TO THE SOURCE

As seen from Earth, Jupiter reaches opposition every 398.88 days, when Sun–Earth–Jupiter are approximately aligned. At this point, both the distance and the frequency of the wave are nearly constant. After 199.44 days, conjunction occurs, and again f_{wave} is constant.

During the interval from solar conjunction to opposition, Earth moves toward Jupiter, and the Doppler effect produces a blueshift of the 56 μHz spectral line. From opposition to the next solar conjunction, Earth moves away from Jupiter, resulting in a redshift. To display the variation of f_{wave} as a function of time, we ignore Jupiter's moons, insert the values from Table 1 into equation (2), and obtain Fig. 3.

Converting the fractional parts of a year into calendar days yields excellent agreement:

$X_1 = 0.9021 \rightarrow$ 2000 November 25. The astronomical opposition occurs on 2000 November 28.

$X_2 = 1.992 \rightarrow$ 2001 December 28. The astronomical opposition occurs on 2001 December 31.

We have no doubt that the wave analyzed here is generated by Jupiter, because f_{wave} always returns to its long-term mean value whenever Jupiter is either in opposition or in conjunction with Earth.

7. SPEED OF THE WAVES

The Doppler effect is a fundamental principle of astronomy and describes the relationship between the frequency shift Δf of the signal and the speed between transmitter and receiver. If we assume that the signal propagates at the speed of light c, we have to use the relativistic equation

$$\Delta f = f_{wave} \cdot \left(\sqrt{\frac{c+v}{c-v}} - 1 \right) \approx f_{wave} \cdot \frac{v}{c} = f_{wave} \cdot 10^{-4} \tag{4}$$

where v is the relative speed between the source and the Earth. For the source Jupiter, the Earth's relative speed oscillates in the range -30 km/s $< v <$ 30 km/s. This limits the Doppler shift to the range $|\Delta f| < 5.6$ nHz. The actual frequency deviation of 71.34 nHz exceeds this limit by a factor of 12.7 (see Fig. 3).

Since the Doppler effect applies and produces the observed frequency shift Δf, we compute $v_{wave} \approx 23.5 \times 10^6$ m/s. This value was determined by comparison with Earth's orbital velocity and may apply only at a distance of 1.5×10^{11} m from the Sun.

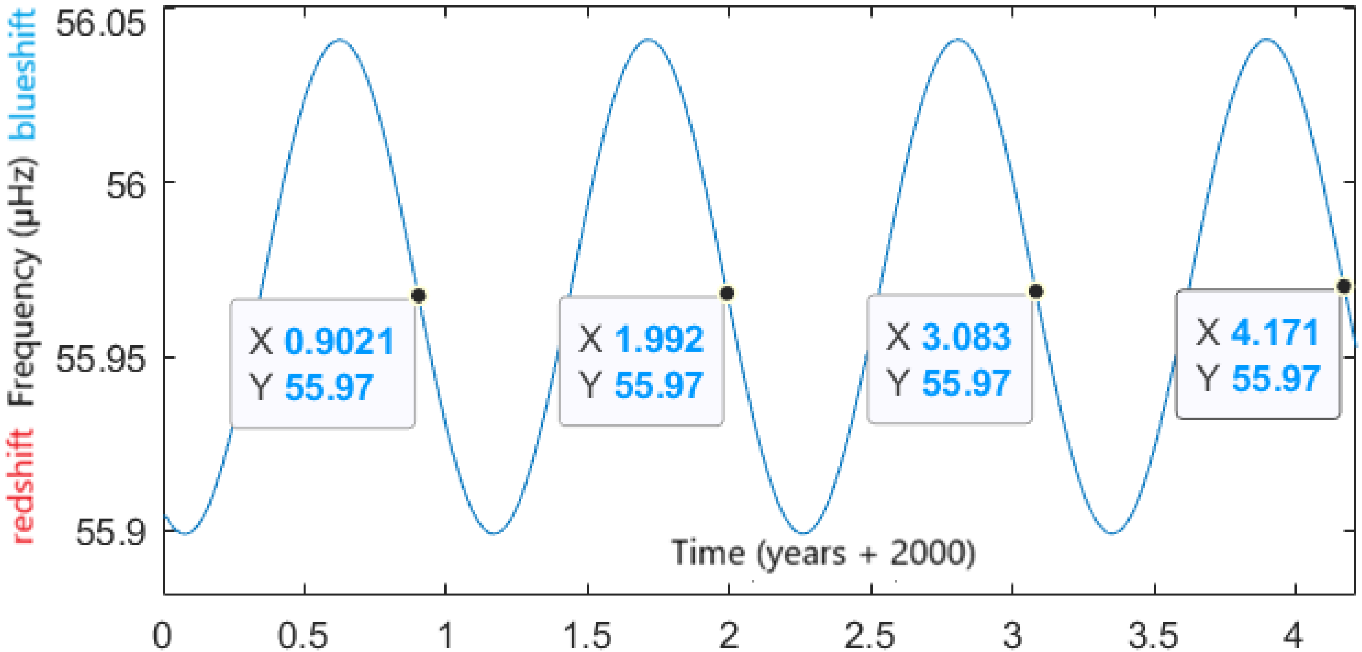

Figure 3. Frequency of Jupiter's wave from 2000 to 2004, computed by inserting only the Earth–Jupiter modulation into equation (2) while intentionally ignoring the moons. The frequency reaches its long-term mean value whenever Jupiter is in opposition or conjunction. The largest deviation from the mean defines Δf.

The average propagation speed of the signal between Jupiter and Earth may differ from this. To answer this question, one would need to compare the phases of the four moons listed in Table 1 with the phases obtained from optical astronomy. Addressing this task lies beyond the scope of this paper.

8. MYSTERIOUS FINE SPECTRUM

We use a direct-conversion receiver consisting of two successive stages. First, we mix the unprocessed signal ensemble down to 0 Hz, limit the bandwidth to 0.6 μHz, and then shift the frequency to $f_{IF-a} \approx 1$ μHz, an arbitrary value for the first intermediate frequency. This procedure corresponds exactly to the standard method described by Weaver (1956). Although this intermediate step is not strictly required, we include it to reduce computation time through a subsequent decimation by a factor of 64.

We then lower f_{IF-a} by applying the Weaver method a second time, obtaining $f_{IF-b} \approx 200$ nHz, narrow the bandwidth to 1 nHz, and measure the amplitude. These steps are repeated 400 times until stable modulation results are achieved.

It is instructive to examine the spectrum around f_{IF-a} shortly before the end of the iterations. In Fig. 4, the carrier frequency of the wave rises above the noise with an SNR of 100 because Jupiter is relatively nearby. We observe two sets of symmetric companions:

$f_{IF-a} \pm 2$ nHz, a consequence of the 20-year record length?

$f_{IF-a} \pm 29$ nHz, presumably generated via amplitude modulation and therefore cannot be altered by PM demodulation (see section 9).

All other lines with frequencies below f_{IF-a} are puzzling. They are arranged asymmetrically and therefore cannot be previously unknown modulations of the wave. Regardless of which barometers we select, these lines always appear with the same frequencies and amplitudes. Varying the values of f_{IF-a} and the bandwidth reveals no comparable cluster of spectral lines at larger frequency offsets.

Could these additional lines be caused by tidal waves in Jupiter's atmosphere? Or do adjacent cloud bands rotate with precisely defined frequencies (differential rotation)? The sources rotate more slowly than Jupiter's solid core and must possess asymmetric mass distributions, since they emit waves. Several observations point to an origin within Jupiter: the amplitudes of all spectral lines in Fig. 4 scale proportionally with the number of planets included in the demodulation. Thus, the sources of these spectral lines lie inside the moon orbits and do not change measurably over the 20-year observation period.

Auclair-Desrotour (2018) proposes the following models:

– Uniformly rotating spherical shells with constant tidal quality factors of $Q \sim 10^3$.

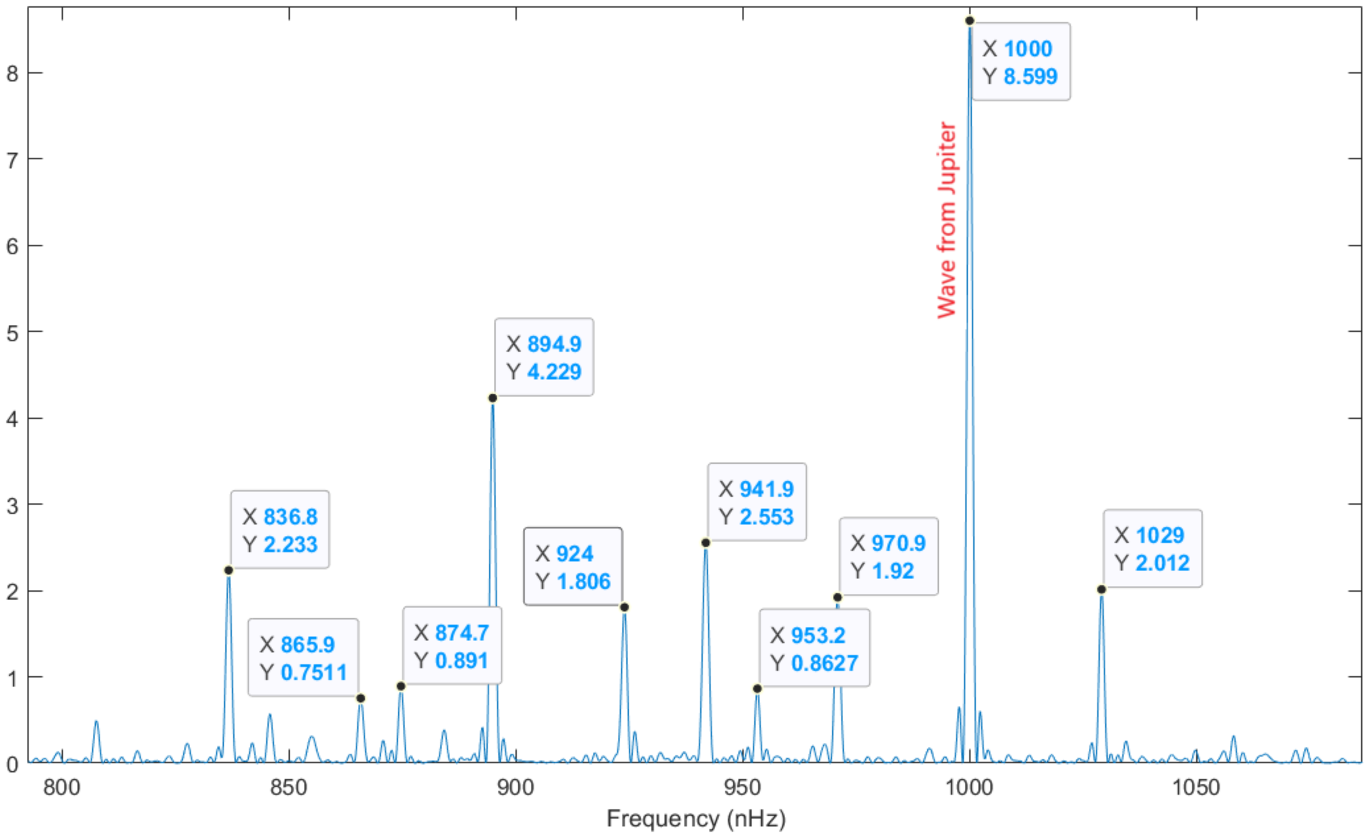

Figure 4. Power spectrum (Welch method) of the IF-a stage after reducing the wave from 56 μHz to 1 μHz and complete phase demodulation. The carrier rises above the noise with an SNR of 100. Two symmetric companion lines appear at ±2 nHz due to the 20-year record length. The two ±29 nHz companions are caused by amplitude modulation of the signal (see Section 9). All additional lines below the carrier are stable across datasets and likely originate from internal oscillators within Jupiter.

– Internal gravito-inertial waves in the period range 1–30 days.

9. PERIODIC VARIATION OF THE SIGNAL AMPLITUDE

All previous results were obtained by exploiting a special property of phase modulation (PM): after demodulation, all sidebands disappear and their energy increases the amplitude of the carrier frequency. This makes it possible to recover PM signals whose sidebands lie far below the noise floor. In contrast, amplitude modulation (AM) can only be deciphered when its sidebands clearly exceed the noise level. The triplet on the right side of Fig. 4 satisfies this condition and may have been produced by AM with a modulation frequency of $f_{mod} = 29$ nHz. A useful indication is that the spectral lines at 970.9 nHz and 1029 nHz are symmetrically arranged around the carrier frequency but cannot be removed by PM demodulation. The mathematical argument is even more conclusive:

An AM signal of frequency f can be written as follows:

$$S_{AM} = A_{carrier} cos(2\pi t f) + \frac{m}{2}(cos(2\pi t(f - f_{mod}) + cos(2\pi t(f + f_{mod})) \tag{5}$$

A PM signal of frequency f consists of many sidebands, the sequence of which begins as follows:

$$S_{PM} = J_0(\eta) cos(2\pi t f) - J_1(\eta)(sin(2\pi t(f - f_{mod}) + sin(2\pi t(f + f_{mod}))) - ... \tag{6}$$

This is not the place to discuss the meaning of the symbols. The crucial point is that *both* modulation methods produce identical sideband frequencies ($f \pm f_{mod}$). The phases (sin(. . .) and cos(. . .), respectively) differ by $\pi/2$. This difference cannot be detected in the spectrum because the spectrum discards all phase information. The PM demodulation method described above detects this difference and ignores all sidebands generated by AM.

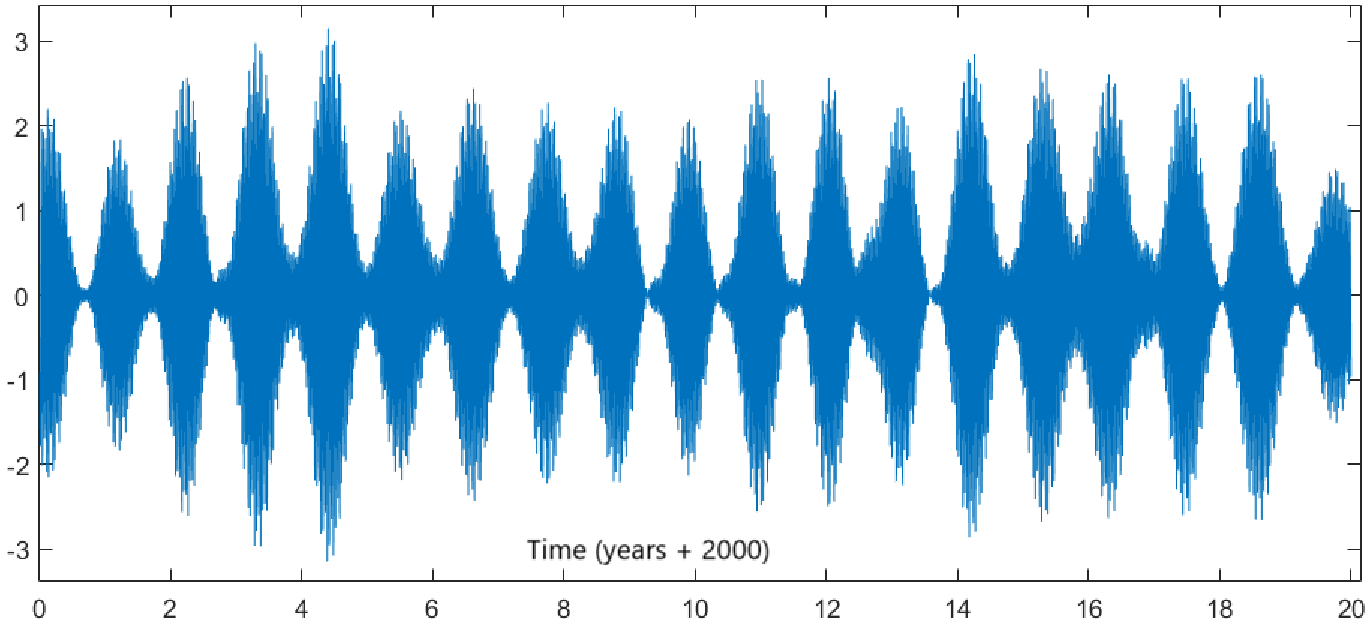

Figure 5. Amplitude modulation of the signal at 56 μHz. Prior to this, the carrier frequency was shifted to 1000 nHz and the bandwidth limited to the range 967 nHz $< f <$ 1033 nHz. The modulation periods are ~397 days and ~12 years, respectively, corresponding to the known orbital periods of the planet Jupiter.

AM can be demonstrated through the phase-coherent addition of the necessary three spectral lines: if all signals outside the bandwidth 967 nHz $< f <$ 1033 nHz are suppressed and all signals within that range are summed, Fig. 5 shows that the signal from Jupiter at 56 μHz is strongly amplitude-modulated.

From the perspective of radio engineering, we can interpret this result as follows: The distance to Jupiter varies between ~4.2 AU and ~6.2 AU. Since the signal amplitude in the far field decreases in proportion to $1/r$, we would expect an AM modulation index of $m \approx 0.68$. Using the values from Fig. 4 and equation (5), we calculate $m = 0.46$. This discrepancy arises because Earth is *not* located in the far field of the 'Jupiter' oscillator.

The outer boundary of the near-field—including the transition zone—is considered to be a sphere with a radius of $R = 2v_{\mathrm{wave}}/f \approx 8 \times 10^{11}$ m $\approx$ 5.5 AU centered on Jupiter, treated as an idealized "point antenna." Within this sphere, the energy flux and the polarization direction of the wave are difficult to define—and this is precisely where Earth is located. There is no existing theory on how to interpret the timing of the maxima and minima of the amplitude modulation.

10. SEARCH FOR POSSIBLE SOURCES OF ERROR

We checked weather our procedure contains critical steps that could distort our results:

Wrong sampling: The barometers at the DWD stations measure air pressure every 10 minutes with automatic plausibility checks. The data then pass through several stages of quality control: physical limits, step-change tests, comparison with neighboring stations, comparison with model fields, detection of sensor faults, icing. Only validated values enter the averaging process. The hourly value is not simply 'the instantaneous pressure at 12:00', but a physically corrected, smoothed value. The procedure acts like a low-pass filter with a cutoff frequency of approximately 300 μHz. This may produce a small phase shift in the frequency range around 56 μHz, but it cannot generate a reproducible spectrum.

Aliasing: From the sampling period $T_s = 3600$ s it follows that 'ghost' signals may appear in the spectrum which actually lie above the Nyquist frequency (about 139 μHz) and are 'mirrored' downward. In our case, signals at $f_{alias} \approx 222$ μHz could in principle interfere with the desired signal at 56 μHz. This interference is unlikely:

Jupiter's wave signal is not visible in the spectrum of Fig. 1, and therefore lies below the noise level.

A log-log representation of Fig. 1 shows that the mean amplitude of the air-pressure spectral lines decreases proportionally to f^{-2} (Brownian noise). A signal near f_{alias} would have to exceed the noise by a factor of 16 in order to produce a disturbing alias at 56 μHz. This also applies to the sidebands shown in Fig. 2.

A targeted analysis using datasets with higher sampling frequency shows that the region around f_{alias} is particularly noise-free and contains no identifiable spectral lines.

FFT, Leakage: We do not use (Hann) windows to shape the temporal amplitude profile of the signal mixture. We do not use an FFT to analyze or modify the signal. Therefore, any discussion of whether windowing, leakage, sideband mis-identification, or zero-padding might influence the data processing is unnecessary.

False positives: A *false positive* is a spurious detection: the algorithm reports a signal even though no physical signal is present. In our context, a *false positive* denotes a modulation pattern that maximizes the carrier amplitude but does not correspond to Jupiter's physical Doppler signature. The possibility of false positives can never be excluded absolutely.

We verified that the wave amplitude is proportional to the number of coherently summed barometers (only 20 instead of the usual 40 sensors). Result: OK.

After fully demodulating a dataset (after 400 iterations), we check whether the amplitude of the carrier frequency has approximately the same value as in other datasets. Result: OK.

If the barometer data are replaced by noise, the amplitude of the carrier frequency drops to at most 20 per cent of the value obtained with 'real' data. The modulations are not reproducible, and the characteristic parameters drift aimlessly.

The most important criterion is that the frequency and phase of a real modulation must not change uncontrollably. If f_{mod} leaves the narrow corridor of $\pm 10^{-5} \cdot f_{mod}$ during 200 iterations, we reject that modulation. The only exception is Callisto, presumably due to its conspicuously small modulation index.

The phases of the four moons are hardly predictable. They must stabilize within the first 40 iterations and then assume a value between 0 and 2π. They may deviate from this value by at most ± 0.5. Both criteria react sensitively to changes in the data source (switching barometers). The results in Table 1 are based on a total of 318 iterations on two different computers – without a single outlier.

Several control tests using 'incorrect' frequencies (more than ± 0.2 μHz deviation from f_{wave}) produced no reproducible results.

11. DISCUSSION

Our analysis achieves all primary objectives and provides new insight into Jupiter's internal dynamics. The recovered carrier frequency near 55.97 μHz agrees with the value expected from Jupiter's rotation, but the measured long-term drift reveals that the strongest oscillator – presumably the solid core – does not rotate at a perfectly constant rate. The wave is modulated by the synodic Earth–Jupiter period of 398.88 days, causing the frequency to oscillate around its mean value. The carrier consistently returns to this mean whenever Jupiter is in opposition or conjunction, confirming the planetary origin of the signal.

The wave exhibits multiple phase modulations corresponding to the orbital periods of the four Galilean moons. Io produces an unexpectedly large modulation index, consistent with the strong tidal forcing expected from the 4:2:1 Laplace resonance among Io, Europa, and Ganymede. Callisto's much smaller modulation index suggests that the outer moon contributes only weakly to Jupiter's deformation. Despite extensive searches, no additional stable modulation frequencies were found over the 20-year interval.

The demodulated spectrum reveals further narrow lines that cannot be attributed to known tidal forcing or instrumental effects. Their amplitudes scale with the number of coherently summed barometers, and they remain stable across all datasets, indicating an origin within Jupiter. These lines may arise from internal gravito-inertial waves or from rotating, non-axisymmetric shells beneath the cloud layer. The absence of dispersion across the 20–90 μHz range implies that all spectral components propagate at the same speed, consistent with a coherent wave field.

Extensive control tests rule out sampling artifacts, aliasing, FFT leakage, and false positives. Incorrect modulation frequencies fail to produce reproducible results, whereas correct frequencies converge rapidly and remain stable. The robustness of the modulation parameters across 318 independent realizations demonstrates that Earth's atmosphere responds coherently to Jupiter's microhertz wave field.

12. CONCLUSION

The detected microhertz waves exhibit stable frequencies, well-defined modulation patterns, and a propagation speed of approximately 23.5×10^6 m/s. Although this speed differs substantially from the speed of gravitational waves predicted by general relativity, the observed signal is nonetheless of planetary origin. The carrier frequency and its modulations consistently track Jupiter's orbital geometry, and the wave returns to its mean value at each opposition and conjunction.

The results indicate that Jupiter hosts multiple internal oscillators with distinct frequencies, concealed beneath its cloud cover. The strongest oscillator – likely the solid core – exhibits measurable long-term drift. Additional spectral lines suggest the presence of rotating, non-axisymmetric shells or internal gravito-inertial modes. Preliminary measurements of Saturn show only a single dominant oscillator, hinting at structural differences between the two giant planets.

These findings demonstrate that long-term atmospheric pressure records can serve as coherent detectors for microhertz waves generated by nearby planets. Future work should compare the measured moon phases with optical ephemerides and extend the analysis to other planetary systems.

13. AVAILABILITY OF PROGRAMS AND DATA

The Deutscher Wetterdienst (2021) stores historical measurement results from German weather stations (raw data). The error-corrected barometer files are also available from the author upon request.

The homodyne detection code was written in MATLAB R2020a. The code (Jupiq8c.m and JupRichtung.m) is available in the github repository:
https://github.com/herbertweidner/cGW/tree/main

https://github.com/herbertweidner/Jupiter/tree/main

The programs will be explained by the author upon request.

REFERENCES

Auclair-Desrotour P., Leconte J., 2018, Semidiurnal thermal tides in asynchronously rotating hot Jupiters, A&A 613, A45, https://doi.org/10.1051/0004-6361/201731683

DWD, 2021, https://opendata.dwd.de/climate_environment/CDC/observations_germany

Hartmann T., Wenzel H., 1995, The HW95 tidal potential catalogue, https://publikationen.bibliothek.kit.edu/160395, https://doi.org/10.1029/95GL03324

Küpfmüller K., Kohn G., 1993, Theoretische Elektrotechnik und Elektronik: Eine Einführung, ISBN 978-3540565000

Weaver D., 1956, A third method of generation and detection of single-sideband signals, Proceedings of the IRE, 1956, pp. 1703-5.